Amplitude-frequency dependencies of wave attenuation in single-crystal quartz: Experimental study

E. I. Mashinskii[1]

Received 24 March 2008; revised 3 July 2008; accepted 14 August 2008; published 11 November 2008.

[1] The experiments have been conducted to investigate the effect of strain amplitude and frequency on the compressional and shear wave attenuation in quartz samples of three types: the intact quartz, fractured quartz, and smoky quartz. The measurements were performed using the reflection method on a pulse frequency of 1 MHz with changing strain in the range $0.3 \leq \varepsilon \leq 2.0$ μstrain under a confining pressure of 10 MPa and at ambient temperature. The essential difference in amplitude-frequency characteristics of wave attenuation in three quartz types has been detected. The intact quartz shows the more "simple" behavior in comparison with the fractured and smoky quartz. The attenuation (the inverse quality factor Q) depends on strain amplitude as $Q^{-1}(\varepsilon) \sim \varepsilon^{-n}$, where $n \cong 0.005-0.085$, with the greatest decrease in the smoky and fractured quartz reaching of about 15%. Relaxation spectra of attenuation are presented in the frequency range from 0.4 to 1.4 MHz. The dependence $Q_p^{-1}(f) \sim f^{-1.2}$ characterizes the intact and fractured quartz, whereas the smoky quartz has the relaxation peak. The dependence $Q_s^{-1}(f) \sim f^{-0.84}$ presents S wave relaxation spectrum in the intact quartz; in the fractured and smoky quartz, the attenuation peaks take place. The strain amplitude variation exerts influence on the relaxation strength, the peak frequency, and the width of the relaxation peak. Such behavior of attenuation can be explained by a joint action of viscoelastic and microplastic mechanisms. These results can be considered as a contribution for providing the experimental background to the theory of attenuation in rocks. They can also be used in solving applied problems in material science, seismic prospecting, etc.

Citation: Mashinskii, E. I. (2008), Amplitude-frequency dependencies of wave attenuation in single-crystal quartz: Experimental study, *J. Geophys. Res.*, *113*, B11304, doi:10.1029/2008JB005719.

1. Introduction

[2] The wave attenuation is caused by the dissipation of strain energy as seismic waves propagate through an anelastic medium. The knowledge of the anelastic properties of minerals is important for understanding attenuation mechanisms in rocks. One of the manifestations of anelasticity is the dependence of seismic parameters on strain amplitude. The influence of strain amplitude on wave velocity and attenuation in rocks was studied by many researchers [*Mavko*, 1979; *Johnston and Toksoz*, 1980b; *Winkler et al.*, 1979; *Stewart et al.*, 1983; *Murphy et al.*, 1986; *Tutuncu et al.*, 1994a, 1994b, 1998; *Johnson et al.*, 1996; *Ostrovsky and Johnson*, 2001]. A majority of results was obtained with using a longitudinal resonant bar method at the frequencies of 1–20 KHz in the range 0.01–10 μstrain and only some of them through a pulse transmission technique at frequency of about 1 MHz in the same strain range. Data of these studies show that the increase in strain amplitude causes the decrease in wave velocity and the increase in attenuation. There are also some facts that show the contrary situation when the increase in strain amplitude leads to the increase in wave velocity and the decrease in attenuation [*Johnston and Toksoz*, 1980a; *Mashinskii et al.*, 1999; *Mashinskii and D'yakov*, 1999; *Mashinskii*, 2004; *Zaitsev et al.*, 1999]. This is supported by data of the indirect experiments in which both the increase and the decrease in modulus with stress were detected; it was supposed that these dependences were due to microplastic process in rocks [*Mashinsky*, 1994; *Mashinskii*, 2001, 2005b].

[3] A subsequent study with the use of the pulse transmission technique in the restricted amplitude-frequency-pressure space (the strain range 0.3–3 μstrain, the frequency band 0.4–1.4 MHz, constant pressure and temperature) showed some unusual effects. Variation in amplitude in the range 1–3 μstrain causes both a decrease and an increase in V_p and V_s in Madra dolomite under constant uniaxial stress up to 60 MPa [*Mashinskii*, 2004]. A significant decrease in wave attenuation due to an increase of amplitude in the range 0.3–2 μstrain is detected in sandstone and smoky quartz under confining pressure of 20 MPa in the band of 0.4–1.4 MHz [*Mashinskii*, 2005a].

[1]Institute of Petroleum Geology and Geophysics, Siberian Branch of the Russian Academy of Science, Novosibirsk, Russia.

Copyright 2008 by the American Geophysical Union.
0148-0227/08/2008JB005719$09.00

[4] The frequency dependencies of wave attenuation in rocks are usually studied at constant strain amplitude. In the amplitude-frequency-pressure space indicated above, these characteristics, for dry and saturated sandstones, look like linear functions having a relaxation peak [*Winkler and Plona*, 1982; *Winkler*, 1983, 1985; *Spencer*, 1981]. Relaxation peaks were also detected in a clay-containing sandstone [*Tutuncu et al.*, 1994a] and even in lucite [*Prasad and Manghnani*, 1997]. A joint consideration of the effect of strain amplitude and frequency in the same phase space revealed an unusual influence of variable strain amplitude on the relaxation spectra of attenuation [*Mashinskii*, 2006, 2007]. Variation in strain amplitude causes the shift of the attenuation peak in the frequency domain, the change in the width of relaxation peak, and others.

[5] A study of wave attenuation with taking into account the joint influence of strain amplitude and frequency factors is of interest not only as a scientific problem. New effects can be useful to improve the diagnostic methods of solving applied problems of material science, acoustic logging, seismic prospecting and others [*Dvorkin et al.*, 2003; *Mavko and Dvorkin*, 2005; *Zaitsev and Matveev*, 2006].

[6] The paper presents an experimental study of the influence of strain amplitude on the relaxation spectra of wave attenuation in the intact, fractured and smoky quartz. This work has been performed in the development of my previous works [*Mashinskii*, 2006, 2007]. A distinctive feature of this work from the previous ones dealing with polycrystals is the joint study of the strain amplitude and frequency effects in single crystals of different types.

2. Experimental Configuration and Methodology

[7] The experiments were conducted with using the pulse transmission technique at varying strain amplitude in the range (0.3–2.0) μstrain under constant confining pressure and ambient temperature. Three types of quartz (intact, fractured and smoky) were used. Quartz was taken for the study because sandstone as a petroleum-gas reservoir rock consists mainly of quartz. As expected, quartz is one of "simpler" natural materials. Anelastic characteristics of a such solid prove useful for understanding the behavior of more complicated materials.

[8] The sample is a bar carved from a natural druse. Quartz does not have subgrains. There are free dislocations and heterogeneities in the form of pores and inclusions. Sizes of pores reach 200 μm, and they are filled by firm-phase material in the form of debris and angular fragments. Chemistry of inclusions in the fractured quartz is similar (SiO_2) and smoky quartz contains many chemical elements. The density of heterogeneities and defects is high. Intact quartz is optically transparent and the fractured quartz is optically opaque. Crystallographic orientation for intact and fractured quartz crystals within the apparatus is the same and smoky quartz has arbitrary orientation. The sample is a cylinder of 2 cm in length and 4 cm in diameter. The density of quartz is 2.6 g cm^{-3}.

[9] The experimental configuration is shown in Figure 1a. A pulse transmission type technique is used. The transducer/sample assembly is the identical apparatus as used by *Jones* [1995] and *Winkler* [1983]. It is three-layer model. The first and third layers are of cylinder form and are made of beryllic bronze. It provides the identical reflection of waves on sample boundaries. The first layer performs a role of the delay line and the third layer is the acoustic load. The rock sample is between these layers. Excitation and reception of ultrasonic pulses (f $\approx$ 1 MHz) are carried out by means of the piezoelectric elements that are rigidly fixed on the acoustic delay layer. The transducer is polarized on a compressional and shear wave. Each transducer is combined as the source-receiver's pair providing the excitation and reception of P or S wave. The confining pressure of 10 MPa provides a constancy of contact conditions on borders of the layer. *Jones* [1995] showed that measurements of Q with using this technique can be made reliable for confining pressure higher than $\sim$5 MPa since, in this case, the degree of coupling between the rock sample and buffer rods is sufficient for providing a stiff contact. Nevertheless, the reflection method for measuring the nonlinear properties of rocks requires for the buffer rods to be in a welded contact with the rock sample. Therefore, we used the fluid couplant at all interfaces. *Spencer* [1981] showed also that a thin film (for example, the epoxy) for the bond (<0.1 mm) has a negligible effect on the measurements. Interference from sidewall reflections due to finite size of the samples is to be negligible above 0.5 MHz [*Jones*, 1995]. As shown by *Winkler and Plona* [1982], data below 400 kHz should be discarded because of uncorrected diffraction effects. The same advice is given by *Stewart et al.* [1983]: the lower end of frequencies should be restricted to the frequencies above $\sim$0.4 MHz to avoid problems associated with ultrasonic beam diffraction. Therefore, we used the frequency band $\Delta f_{\text{min-max}}$ = 0.4–1.4 MHz for study the relaxation spectra of attenuation. Frequency characteristics of attenuation are determined using spectral ratio method and graphed for every strain-amplitude level.

[10] The attenuation is calculated by using the relation [*Winkler*, 1983]

$$Q^{-1} = \alpha V/8.686\pi f = \alpha\lambda/8.686\pi, \tag{1}$$

where α is the attenuation coefficient in dB m^{-1}, V is the phase velocity in m s^{-1}, and f is the frequency in Hz. The value of α is calculated using the relations [*Winkler and Plona*, 1982]

$$\alpha(\omega) = \frac{8.686}{L}\ln\left[\frac{|R_{23}|A_{top}(f)}{|R_{12}|A_{bot}(f)}(1 - R_{12}^2(f))\right], \tag{2}$$

where L is twice the sample thickness (in m), $A_{top}(f)$ is the Fourier magnitude of the reflected pulse from the front of the sample (top buffer/sample interface), $A_{bot}(f)$ is the Fourier magnitude of the reflected pulse from the back face of the sample (bottom sample/buffer interface), $R_{12}(f)$ is the reflection coefficient at the interface between the coupling buffer and the sample, and R_{23} is the reflection coefficient at the interface between the sample and the backing buffer. In our case, the coupling and backing buffers are identical (beryllic bronze), and, therefore, $R_{12}(f) = -R_{23}(f)$. The coefficient $R(f)$ is calculated as

$$R(f) = \frac{\rho_r V_r(f) - V_b\rho_b(f)}{\rho_r V_r(f) + \rho_b V_b(f)}, \tag{3}$$

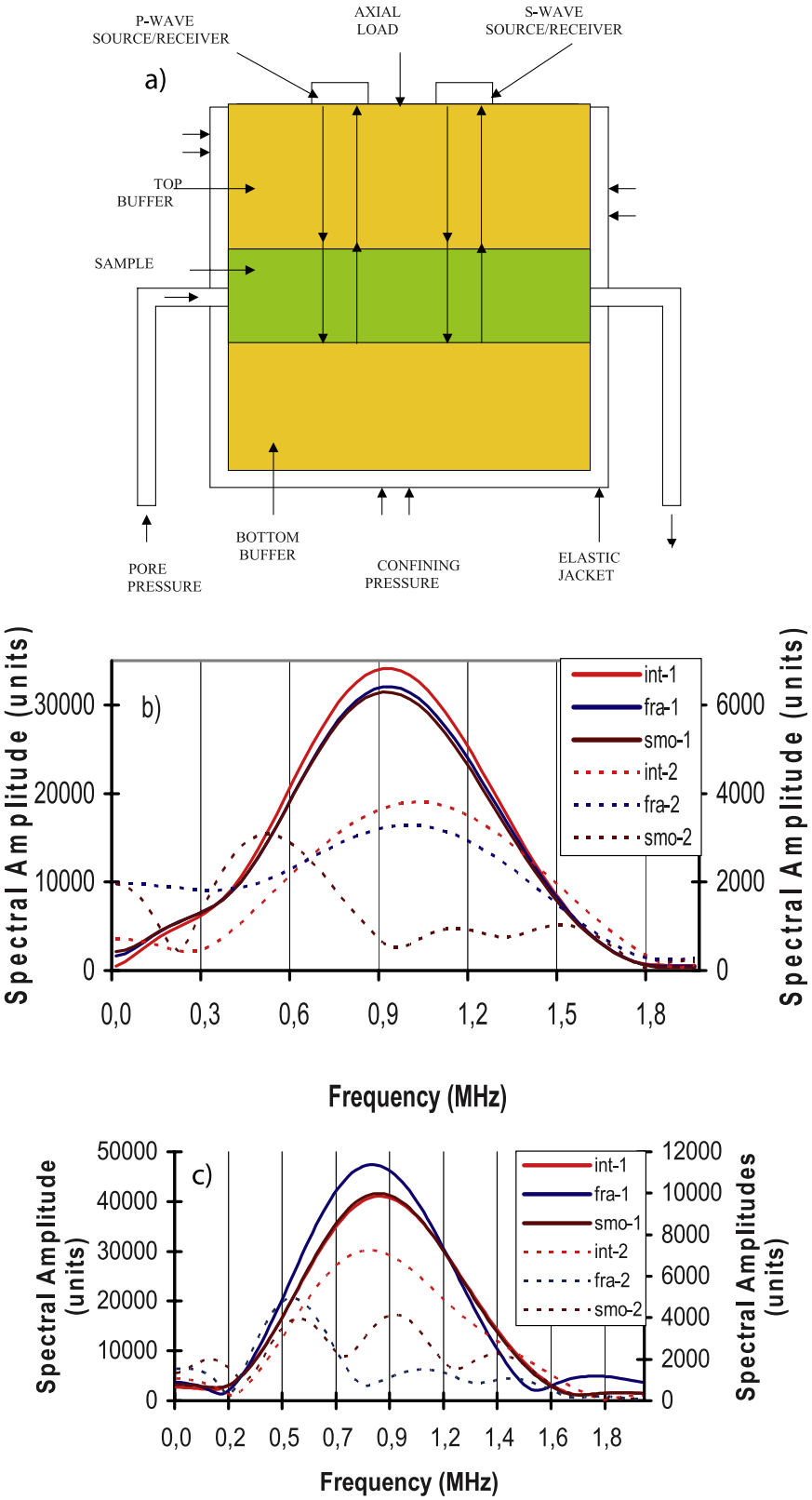

Figure 1. (a) The experimental configuration. (b) and (c) Fourier spectra of the incident (solid line) and the second reflected (dashed line) pulse of compressional (Figure 1b) and shear (Figure 1c) wave for maximum strain amplitude in the intact, fractured, and smoky quartz.

where ρ_r, ρ_b are the densities and $V_r(f)$, $V_b(f)$ are the velocities in the sample and the beryllic bronze buffer rod, respectively.

[11] Measurements are conducted at a varying strain amplitude over the closed cycle under all other conditions being invariable. The amplitude change is discrete from the minimum to the maximum and then back to the minimum: $\varepsilon_{\min} = \varepsilon_1 \rightarrow \varepsilon_2 \rightarrow \cdots \rightarrow \varepsilon_{\max} = \varepsilon_6 \rightarrow \cdots \rightarrow \varepsilon_1$, namely, $\varepsilon_1 = 0.3$, $\varepsilon_2 = 0.5$, $\varepsilon_3 = 1.0$, $\varepsilon_4 = 1.3$, $\varepsilon_5 = 1.7$, and $\varepsilon_6 = 2$ ($\times 10^{-6}$, i.e., microstrain). Thus the closed cycle ($\varepsilon_1 \rightarrow \varepsilon_6 \rightarrow \varepsilon_1$) includes 11 amplitude magnitudes (six upward and five downward). The measurement of attenuation is made at each amplitude level. The attenuation spectra are calculated for each frequency within the bandwidth of the pulse for all strain amplitudes.

[12] An accurate estimation of strain amplitude is difficult. First, we make a rough estimate using expression [*Johnson et al.*, 1996]: $\varepsilon_M = \langle\varepsilon\rangle_t = 2\langle\ddot{u}\rangle_t/L_0\omega^2$, where $\langle\ddot{u}\rangle_t$ is time-averaged acceleration, ω is the angular frequency, and L_0 is the bar length at rest. Second, for the pulse propagation, the strain amplitude is estimated relative to the wavelength λ instead of the bar length L_0. Then: $\varepsilon_M = v/V = 2\pi u/\lambda$, where v is a particle velocity. The strain calculated from both formulas is approximately the same. The displacement u was estimated using the transmission coefficient of piezoelectric transducer at the source voltage. The strain interval is approximately 10^{-7}–10^{-6}. In this work, an accurate estimate of strain amplitude is not obligatory: an order of magnitude is important. Relative change of the attenuation with increasing strain amplitude (under other conditions being constant) is studied.

3. Results

3.1. Fourier Spectra

[13] P and S wave Fourier spectra of reflections from the front and back faces of the sample (its top and bottom interfaces) in the intact, fractured and smoky quartz are presented in Figures 1b and 1c. To study the influence of strain amplitude on P and S waves, the spectra A^P_{top}, A^P_{bot}, A^S_{top}, A^S_{bot} are plotted for varying strain amplitude values. The upward ($\varepsilon_1 \rightarrow \varepsilon_6$) and downward ($\varepsilon_6 \rightarrow \varepsilon_1$) Fourier curves practically coincide. For simplification, here are shown only the upward spectra for the maximum strain amplitude. A dominant frequency of the pulse is $f^P_{top} = 0.923$ MHz for P wave, and $f^S_{top} = 0.877$ MHz for S wave.

[14] P wave Fourier spectra, $A^P_{bot}(f)$ together with $A^P_{top}(f)$, are presented in Figure 1b. For the intact and fractured quartz, they are simpler in comparison with those in the smoky quartz. A dominant frequency, f^P_{bot}, changes with increasing strain amplitude. In the intact quartz, f^P_{bot} is higher than f^P_{top} for all strain amplitudes. The same situation takes place in the fractured quartz, except for the minimal strain amplitude. In the smoky quartz, f^P_{bot} is essentially lower in comparison with f^P_{top}. The increase in f^P_{bot} owing to increasing strain amplitude (in the range ε_1–ε_6) is 6%, 13%, and 13% for the intact, fractured and smoky quartz, respectively.

[15] S wave Fourier spectra, $A^S_{bot}(f)$ with $A^S_{top}(f)$, are presented in Figure 1c. For the intact quartz, the spectrum is simple and a dominant frequency is practically constant. For the fractured and smoky quartz, the spectra are more complicated. In the fractured quartz, f^S_{bot} is much lower than f^S_{top}. The spectrum in the smoky quartz has a minor maximum.

3.2. Relaxation Spectra

[16] The dependences of the P wave attenuation in quartz as a function of frequency for the six upward strain amplitudes, $Q_p^{-1}(f, |\varepsilon_{1-6}|_{const})$, are shown in Figure 2a. These are the relaxation spectra of different curve form in the range 0.4–1.4 MHz. The significant segment of the curve $Q_p^{-1}(f, |\varepsilon_n|_{const})$ around f_{top}, looks in the intact and fractured quartz as nearly a linear dependence $Q_p^{-1} \sim f^{-1.2}$. The relaxation spectrum in the smoky quartz contains the attenuation peak on the frequency nearby $f_{att\text{-}peak} = 0.923$ MHz. The increase in strain amplitude moves a peak toward the smaller attenuation and higher frequencies. The decrease in attenuation reaches 15%, the displacement in frequency is small. In the intact and fractured quartz, the strain amplitude does not cause the displacement of the relaxation curve, and therefore, these curves, for principal strain amplitudes (ε_2–ε_6), coincide.

[17] The dependences of S wave attenuation in quartz as a function of frequency $Q_s^{-1}(f, |\varepsilon_{1-6}|_{const})$ for the six upward strain amplitudes are presented in Figure 2b. The relaxation spectrum in the main presents a straight line as $Q_s^{-1} \sim f^{-0.84}$. The relaxation spectra in the fractured and smoky quartz contain the main attenuation peak on $f_{att\text{-}peak1} = 0.815$ and 0.692 MHz and a minor peak on $f_{att\text{-}peak2} = 1.23$ and 1.169 MHz, respectively. Strain amplitude practically does not influence on the relaxation spectrum in the intact quartz. Relaxation curve in the fractured quartz with increase in strain amplitude moves down toward smaller attenuation and lower frequencies. In the smoky quartz, the increase in strain amplitude leads to the displacement of the peak toward smaller attenuation and higher frequencies.

3.3. Influence of Strain Amplitude on Attenuation Parameters

[18] P and S wave velocities practically do not depend on strain amplitude in the given amplitude range (Figure 3). The exception is the P wave velocity in the smoky quartz. Here a small decrease (of about 1%) is observed in the wave velocity with increasing strain amplitude.

3.3.1. Attenuation on Top Reflection Frequency

[19] P and S wave attenuations versus strain amplitude $Q_p^{-1}(\varepsilon)$, $Q_s^{-1}(\varepsilon)$ for the top reflection frequency (“incident” frequency) under a confining pressure of 10 MPa are presented in Figure 4. The P wave attenuation in the smoky quartz is 2 times greater than that in the fractured and intact quartz: $Q_p^{-1}\langle\text{smo}\rangle \gg Q_p^{-1}\langle\text{fra}\rangle > Q_p^{-1}\langle\text{int}\rangle$. The attenuation in the intact and fractured quartz does not depend on strain amplitude. The attenuation in the smoky quartz decreases with the increase in strain amplitude by 15%. The S wave attenuation in the fractured quartz is greater than in the smoky quartz and especially in the intact quartz: $Q_s^{-1}\langle\text{fra}\rangle > Q_s^{-1}\langle\text{smo}\rangle > Q_s^{-1}\langle\text{int}\rangle$. The increase in strain amplitude causes the decrease in attenuation in the intact, fractured and smoky quartz by 5%, 6%, and 12%, respectively.

3.3.2. Peak Attenuation

[20] As stated above, the individual relaxation spectra have one-two peak and one-two minimum. The first minimum is at the left, and the second minimum is to the right

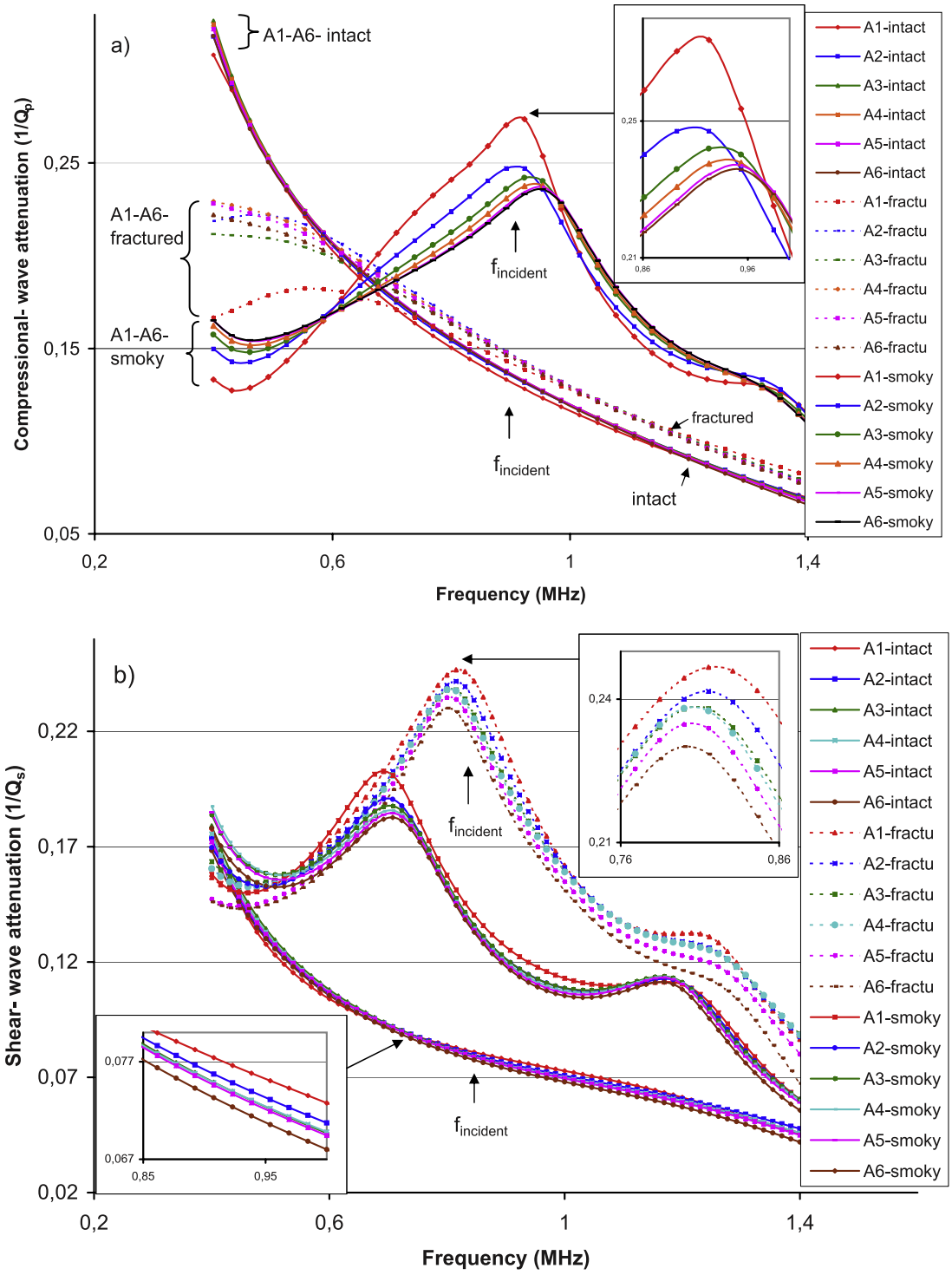

Figure 2. (a) Compressional wave attenuation in the intact, fractured and smoky quartz as a function of frequency for the six upward strain amplitude. (b) Shear wave attenuation in the intact, fractured, and smoky quartz as a function of frequency for the six upward strain amplitude.

of the first peak. The strain amplitude causes changes in the values of peak attenuation (the relaxation strength Δ) and attenuation minimum. Figure 5 shows P wave peak attenuation as functions of strain amplitude, $Q^{-1}_{P\text{-}peak1}(\varepsilon)$, for the smoky quartz. The increase in the strain amplitude causes the decrease in $Q^{-1}_{p\text{-}peak1}$ up to 15%. Figure 5 also shows S wave peak attenuations as functions of strain amplitude, $Q^{-1}_{S\text{-}peak1}(\varepsilon)$, for the fractured and smoky quartz. The attenuations $Q^{-1}_{S\text{-}peak1}\langle \text{fra}\rangle$ and $Q^{-1}_{S\text{-}peak1}\langle \text{smo}\rangle$ monotonically decrease with increasing strain amplitude. The range of deviations in the attenuation values is about 6%. The dependence $Q^{-1}_{S\text{-}peak2}\langle \text{smo}\rangle(\varepsilon)$ is practically absent.

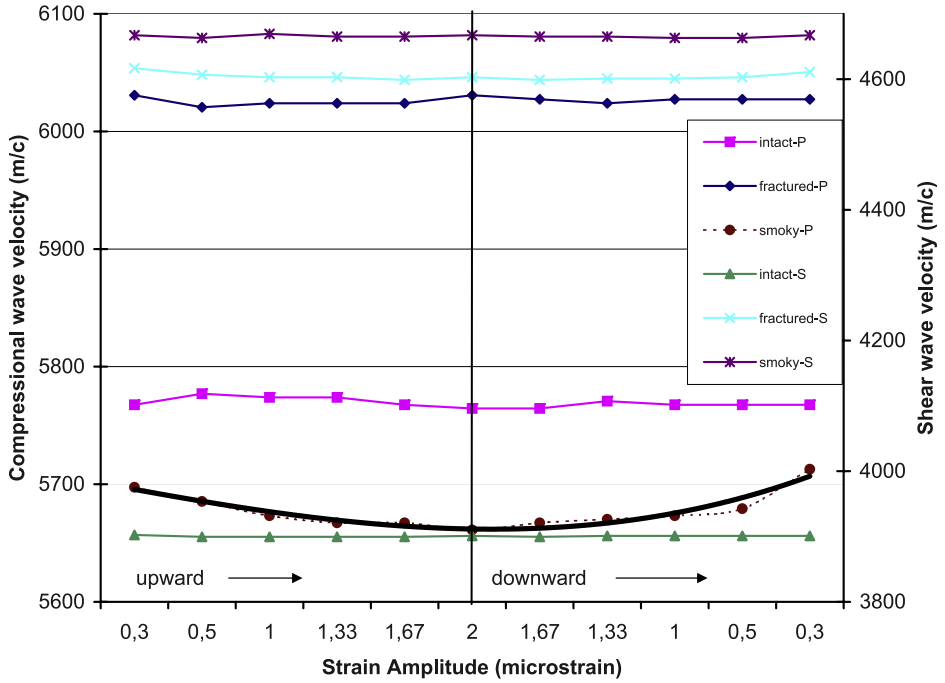

Figure 3. Compressional (solid line) and shear (dashed line) wave velocity in the intact, fractured, and smoky quartz as function of the upward and downward strain amplitude ($\varepsilon_1-\varepsilon_6-\varepsilon_1$). Polynomial approximations for P wave velocity in the smoky quartz are made.

3.3.3. Peak Frequency

[21] The variation in strain amplitude causes the displacement of the peak frequency $f_{att\text{-}peak}$. Changes in peak frequency are small, but it is necessary to mention this fact.

3.3.3.1. Fractured Quartz

[22] The P wave relaxation peak (see Figure 2) exists only on the strain amplitudes $\vec{\varepsilon}_1$, $\bar{\varepsilon}_1$ and $\vec{\varepsilon}_2$, $\bar{\varepsilon}_2$, and it is absent on greater amplitudes. The peak frequency on ε_2 is lower than on ε_1. In this connection, one can be surmised that the relaxation peak for greater amplitudes is situated on lower frequencies outside the given frequency range. Variation in the strain amplitude causes a displacement of S wave peak only on ε_3 but on the other amplitudes the shift is absent. A jump in $f_{att\text{-}peak}$ occurs toward lower frequencies when the

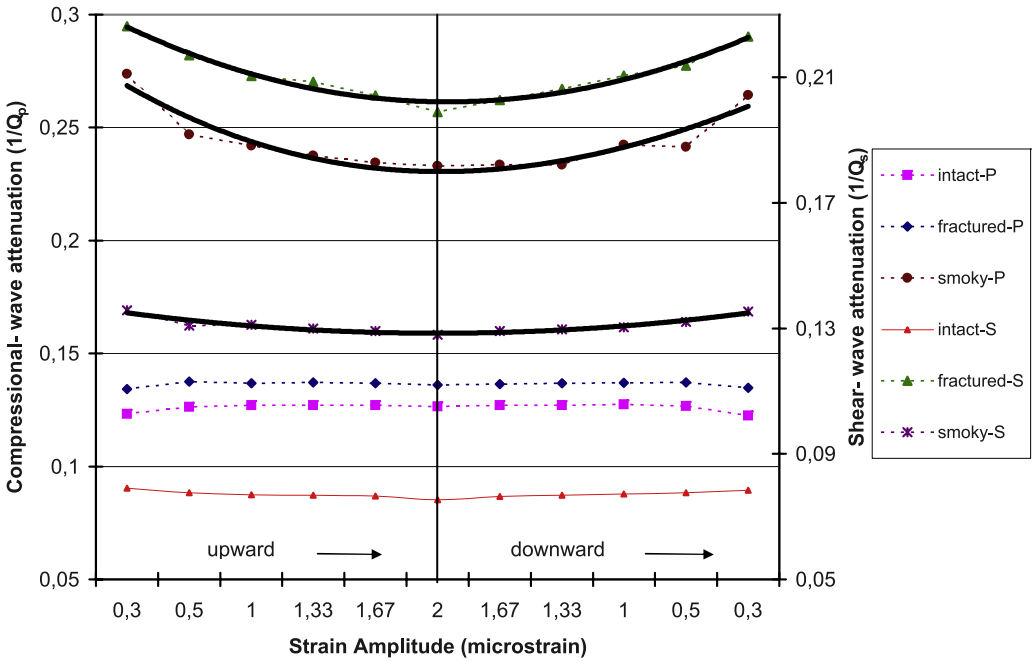

Figure 4. Compressional (solid line) and shear (dashed line) wave attenuation on the incident frequency in the intact, fractured and smoky quartz as a function of the upward and downward strain amplitude Polynomial approximations for the three curves are made.

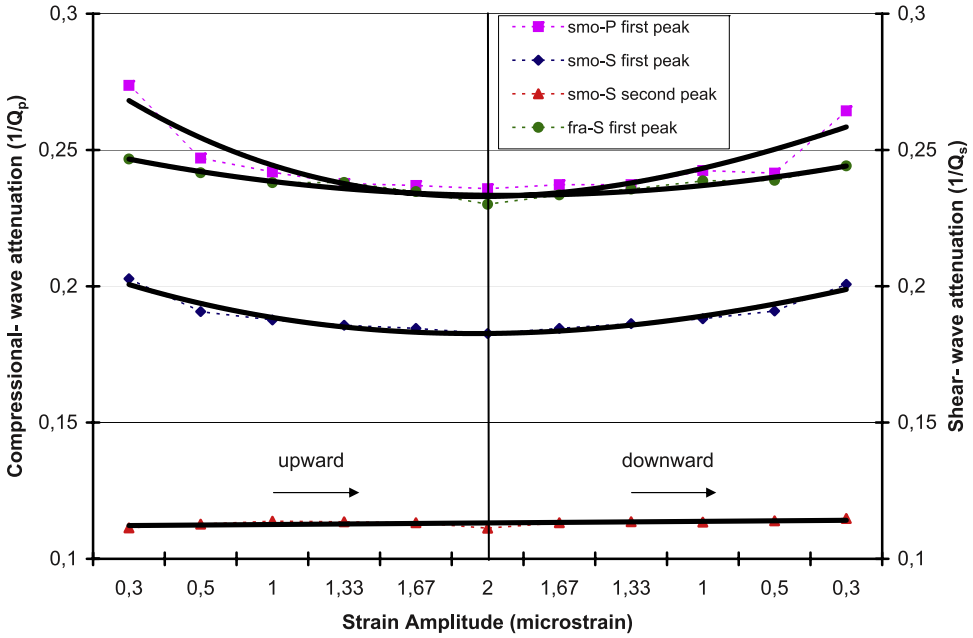

Figure 5. Peak attenuation of P and S wave in the fractured and smoky quartz as a function of the upward-downward strain amplitude ($\varepsilon_1-\varepsilon_6-\varepsilon_1$). Linear and polynomial approximations are made.

amplitude increases and toward higher frequencies when it decreases. The upward and downward peak frequencies practically coincide.

3.3.3.2. Smoky Quartz

[23] For P wave, the jump in $f_{att\text{-}peak}$ occurs toward high frequencies with the increase in amplitude and toward low frequencies with its decrease (see Figure 2). The upward and downward peak frequencies completely coincide. This is an evidence of the high reliability of the result. There are two peaks in the relaxation spectra of S wave attenuation. The frequency $f_{att\text{-}peak1}$ slightly varies and the frequency $f_{att\text{-}peak2}$ remains invariable with variation in strain amplitude.

3.3.4. Width of Relaxation Peak

[24] Variation in the strain amplitude causes diverse changes in the width of the relaxation peak in the fractured and smoky quartz. Figure 6 shows the ratio of the peak width

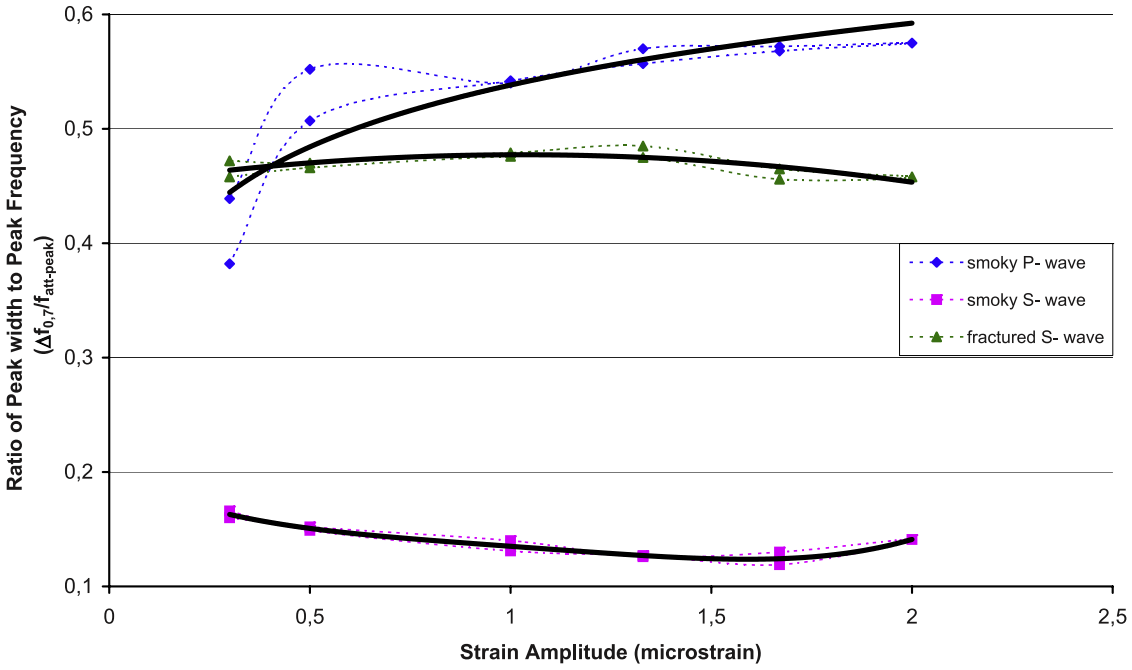

Figure 6. Ratio of the peak width to the peak frequency ($\Delta f_{0.7}/f_{att\text{-}peak}$) as a function of the upward-downward strain amplitude of P and S wave in the fractured and smoky quartz. Logarithmic and polynomial approximations are made.

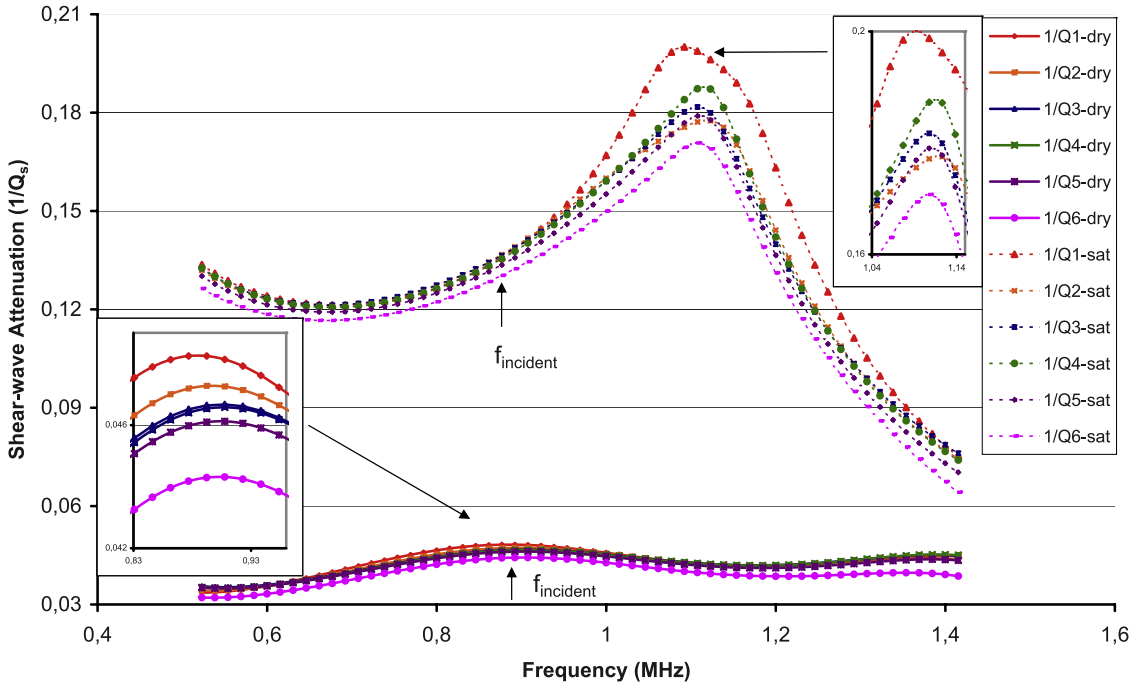

Figure 7. Shear wave attenuation in the dry and saturated sandstone as a function of frequency for the six upward strain amplitudes (ε_1–ε_6). A confining pressure is of 20 MPa (taken from *Mashinskii* [2007]).

$\Delta f_{0.7}$ to the peak frequency $f_{att\text{-}peak1}$ as a function of strain amplitude: $[\Delta f_{0.7}/f_{att\text{-}peak1}](\varepsilon_{1-6-1})$, where $\Delta f_{0.7}$ is the frequency band at 0.7 peak height, $(0.7 \times Q^{-1}_{P,S\text{-}peak1}(f_{att\text{-}peak1}))$. The dependence $[\Delta f_{0.7}/f_{att\text{-}peak1}](\varepsilon_{1-6-1})$ for S wave in the fractured quartz is the domelike curve with deviations of about 6%. The ratio $\Delta f_{0.7}/f_{att\text{-}peak1}$ for P wave in the smoky quartz monotonically increases with increasing strain amplitude; the increase reaches 50%. The ratio $[\Delta f_{0.7}/f_{att\text{-}peak1}](\varepsilon_{1-6-1})$ for S wave in the smoky quartz is the concave curve; the decrease of this ratio equals 28% in the given strain amplitude range.

4. Discussion

[25] The experiments showed that behavior of quartz under the influence of strain amplitude is not such simple as it may seem. The strain amplitude-frequency characteristics of attenuation in the intact quartz are more simple in comparison with those for the fractured and smoky quartz. The wave attenuation in quartz obeys the following rule:

$$Q^{-1}_{p,s} \propto k\varepsilon^{-\tilde{n}}, \tag{4}$$

where k is a dimensionless coefficient and $\tilde{n} \leq 1$. The index $\tilde{n}$ determines the steepness (the slope of the line) of attenuation variation with amplitude. The fractured and smoky quartz show the decrease in wave attenuation with the increase in strain amplitude ($\tilde{n}_{\max} \approx 0.076$), and at the same time, the intact quartz shows a relatively simple reaction, i.e., strain amplitude independence ($\tilde{n} \approx 0$). Such behavior predicts the hybrid relaxation-hysteresis process [*Arzhavitin*, 2004; *Mashinskii*, 2006] and explains the strain amplitude dependence of attenuation by rock microplasticity.

[26] Microplastic process is a potential cause for the amplitude-dependent relaxation time(s). The relaxation spectra of wave attenuation in the imperfect crystal also undergo a modification under the influence of variable amplitude which causes the change in the relaxation strength, in the width of relaxation peak and the displacement of this peak in coordinates Q^{-1} and f. It occurs because the strain amplitude governs the relaxation time and parameters of relaxation peak [*Mashinskii*, 2006]. Intact quartz is characterized by the linearity of the frequency characteristic and the absence of relaxation peak at least in this frequency range. It is significant that there is sameness in the amplitude effects in the imperfect crystal and for example in sandstone (compare Figure 2 with Figure 7 [from *Mashinskii*, 2007, Figure 6]). These facts indicate hereto that, in all probability, in both cases the defectiveness determines the anelasticity and nonlinearity. Quartz can contain diverse defects including lattice defects. Anisotropy also brings difference in the wave velocities and attenuations. The defects, for example, with triclinic symmetry also can potentially lead to anelastic behavior at MHz frequencies.

[27] The assumption about presence of defects in quartz was examined with the help of scanning electron microscopy (SEM). Thin quartz sections were studied on SEM "LEO1430VP" equipped by energy spectrometer "OXFORD." This study showed that the intact quartz is really homogeneous and does not contain structural defects in the form of pores, cracks and inclusions which are accessible for observation by this apparatus. Surveying with the help of backscattered electrons established that the fractured and smoky quartz have heterogeneities in the form of numerous pores and inclusions. Sizes of pores are within 20–200 μm. Pores are filled by firm-phase inclusions, and it is highly

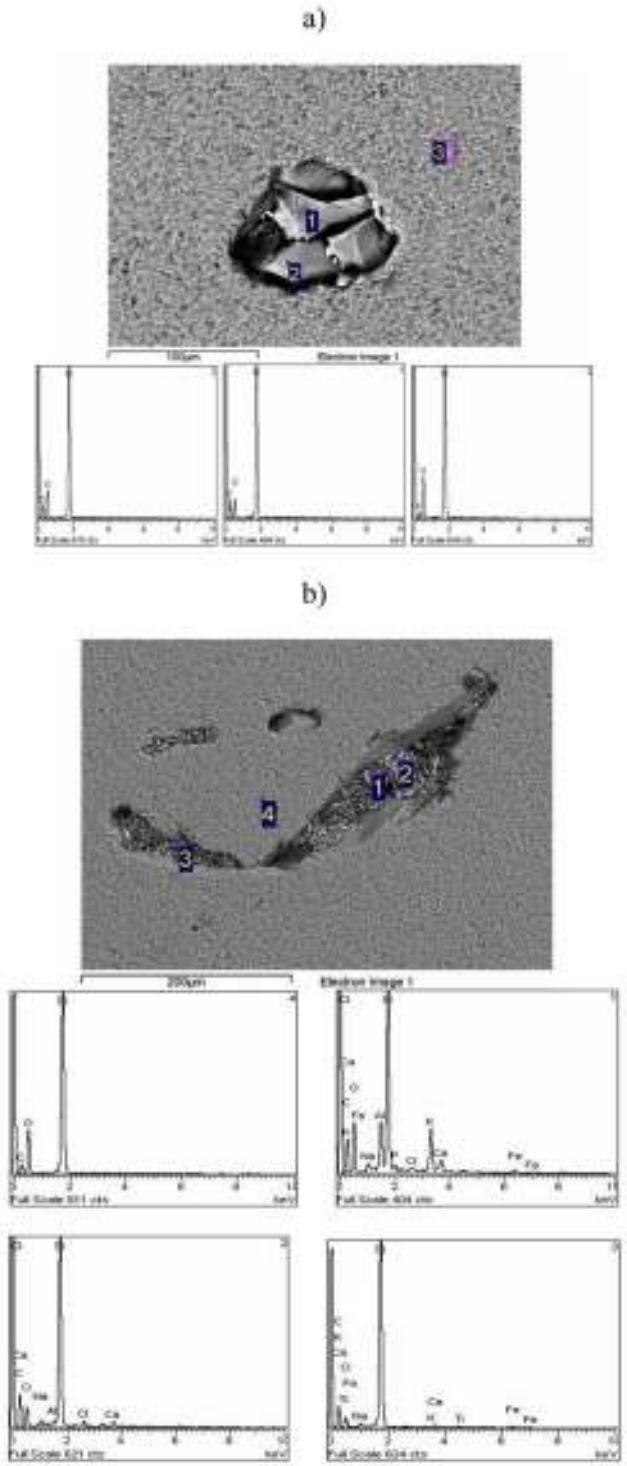

Figure 8. SEM in the (a) fractured and (b) smoky quartz.

probable that they contain a gaseous-liquid phase. The firm-phase inclusions of pores in the fractured quartz consist of quartz (SiO_2), i.e., they have the same chemical constitution as the matrix (see Figure 8a). As distinct from the last, the firm-phase inclusions of pores in the smoky quartz contain also other elements: K, Ca, Al, Na, Fe, Ti (see Figure 8b). Inasmuch as the smoky quartz is more heterogeneous than the fractured quartz and a fortiori the intact quartz, therefore, its anelastic behavior noticeably differs from that of the others. The complementary study with the help of X-ray spectrometry confirms the greater defectiveness of the smoky quartz in comparison with the others. At least, these experiments strengthen the supposition about belonging of defects and heterogeneities to the reason of anelasicity and nonlinearity in the imperfect quartz.

[28] It is necessary to note that an atypical decrease in attenuation versus strain amplitude according to equation (4) is possible theoretically and has definite grounds. The ambiguous dependencies of modulus (wave velocity) on strain obtained from different theoretical models [*Guyer et al.*, 1995; *Guyer and Johnson*, 1999; *Gusev et al.*, 1998] indicate the possibility for such behavior. Besides the indirect prerequisites, there is a theoretical work [*Arzhavitin*, 2004] that predicts not only an increase but a decrease in wave attenuation with increasing strain amplitude.

[29] The relaxation effects governed by strain amplitude require the explanation. The attenuation peak in rocks is usually related to the local fluid flow in the grain boundary space [*Murphy et al.*, 1986]. Systems with solid-solid phase transitions under the influence of strain amplitude can also induce a reaction from one phase to another, causing stress relaxation and an attenuation peak. For example, in the pore-to-pore relaxation model, the peak can be shifted both toward the lower and higher frequencies owing to variation in saturation [*Taylor and Knight*, 2003]. A shift of relaxation peak in dependence on frequency and strain amplitude predicts a nonhysteretic dissipation mechanism described by *Zaitsev and Sas* [2000] and *Zaitsev and Matveev* [2006]. Transformation of the attenuation peak in the amplitude-frequency domain can be explained also using the classical expression for attenuation given as

$$Q^{-1}(\omega) = \Delta \frac{\omega\tau}{1 + (\omega\tau)^2}, \tag{5}$$

where ω is the angular frequency, and τ is the relaxation time given by $1/2\pi f_{att\text{-}peak}$, and Δ is the relaxation strength. The shifts of peak in Q^{-1} and f directions occur because of variations in Δ and τ induced by strain amplitude [*Mashinskii*, 2007]. The relaxation strength Δ in (5) for compressional and shear waves is determined as

$$\Delta_p = \frac{M_u - M_r}{\sqrt{M_r M_u}}, \Delta_s = \frac{G_u - G_r}{\sqrt{G_r G_u}}, \tag{6}$$

where M_u, G_u are the high-frequency compressional and shear modulus, respectively; M_r, G_r are the low-frequency compressional and shear modulus, respectively. The connection between Δ_s and by moduli G_u, G_r is given by the expression [*Jackson et al.*, 2002]

$$G_r/G_u = (1 + \Delta s)^{-1}. \tag{7}$$

Variation of strain amplitude causes the change in the stiffness difference $G_u - G_r$ that leads to the change in Δ and the peak width.

[30] The strain amplitude-dependent shift of the peak frequency can be caused by the change of viscosity and the relaxation time [*Mashinskii*, 2006]. In the case of the

solid-solid boundary, a peak frequency is determined by the relaxation time τ_e [*Jackson et al.*, 2002]

$$\tau_e = \frac{\gamma \eta_b}{G_u \alpha_b}, \tag{8}$$

where η_b is the grain boundary viscosity, G_u is the relaxed shear modulus, $\alpha_b = \delta/d$ is the aspect ratio of the grain boundary region of thickness δ for grain size d, and γ is the numerical factor of order 1. The variation in amplitude leads to the changes in η_b, τ_e, and $f_{att\text{-}peak}$. The grain boundaries in quartz are absent but there are the firm-phase inclusions in pores, which possibly play a part similar to the grain boundaries. In spite of this, it is difficult to draw a well-defined conclusion about this effect without an additional study. In essence, the fact of relaxation process in quartz suggests the presence therein of heterogeneities and defects.

[31] The change in the peak width can also be obtained with the help of the Fuoss-Kirkwood expression [*Cordero et al.*, 2003] that extends the Debye formula (5) by using, for the description of a process, a spectrum of relaxation times

$$Q^{-1}(\omega, T) = \Delta \frac{1}{(\omega\tau)^{\alpha} + (\omega\tau)^{-\beta}}, \tag{9}$$

where $\alpha = \beta < 1$. The parameter α controls the peak broadening in the low-temperature region, where $\omega\tau < 1$, and β does the same in the high-temperature region. In our case, the expression for attenuation (9) can be rewritten in a general formula

$$Q^{-1}(\omega, \tilde{\varepsilon}) = \Delta(\tilde{\varepsilon}) \frac{1}{(\omega\tau)^{\tilde{\alpha}} + (\omega\tau)^{-\tilde{\beta}}}, \tag{10}$$

where $\tilde{\varepsilon}$ is the variable strain amplitude, $\Delta(\tilde{\varepsilon})$ is the strain amplitude-dependent relaxation strength, $\tilde{\alpha}$ and $\tilde{\beta}$ are the amplitude-dependent parameters. The relaxation strength $\Delta(\tilde{\varepsilon})$ is responsible for the value of peak attenuation. The $\tilde{\alpha}$, $\tilde{\beta}$ parameters control the broadening and narrowing of width of attenuation peak thanks to the variable strain amplitude. Such physical process supposes that for the each strain amplitude exists the defined relaxation time and $\tilde{\alpha}$, $\tilde{\beta}$ parameters. Amplitude variation causes the change in the rock characteristics, for example, in viscosity and leads to the variation of relaxation spectrum. It explains the broadening of peak width with increasing strain amplitude that takes place for P wave attenuation in the smoky quartz (see Figure 6).

5. Conclusion

[32] This study has shown that there are many sided aspects of the strain-amplitude influence on the modulus and the relaxation spectra of attenuation. On the one hand, the simplicity of strain amplitude-frequency characteristics of attenuation in the intact quartz convinces that various defects are in charge of anelastic effects. On the other hand, these characteristics show that the relatively simple in structural respect such a solid as quartz behaves in many respects in the same way as the complex structure rock [*Mashinskii*, 2007]. We see that the similar decrease in attenuation under increasing strain amplitude takes place in both cases. These results give grounds to suppose that real quartz presented in many rocks as a main rock-forming mineral can manifest sufficiently anelastic properties even under small strain amplitudes. It can be confirmed by an analogy with olivine-olivine grain boundaries (a region $\leq$1 nm wide) that are able to produce an inelastic attenuation peak [*Faul et al.*, 2004]. The multifarious behavior of peak frequency in dependence on strain amplitude is a new problem for further researches. The amplitude effect is most pronounced in the change in the width of attenuation peak. This fact should be taken into account by the geophysicists specializing on development of seismic methods for search of oil and gas deposits. The defined results have been achieved in this direction using the relaxation effects of Q_p and Q_s from sonic log data for the purpose of distinction of nonreservoir rock from reservoir rock [*Dvorkin et al.*, 2003; *Mavko and Dvorkin*, 2005]. This problem affects the little-known inelastic processes of the small-amplitude wave propagation. The new knowledge about nonlinear-inelastic process during wave propagation will help in discovery of new diagnostic indications permissive to increase the efficiency of seismic method.

[33] **Acknowledgments.** This work was performed with the support of the Russian Fund of Fundamental Researches, grant N 05-05-64709. The author expresses thanks to Y. N. Zanin, A. T. Titov and E. P. Slobotchina for the help in the experimental work.

References

Arzhavitin, V. M. (2004), Amplitude dependence of the internal friction in a Pb-62% Sn alloy, *Tech. Phys.*, *49*(6), 707–710, doi:10.1134/1.1767878.

Cordero, F., A. Paolone, R. Cantelli, and M. Ferretti (2003), Anelastic relaxation process of polaronic origin in $La_{2-x}Sr_xCu_{O4}$: Interaction between charge stripes and pinning centers, *Phys. Rev. B*, *67*, 104508, doi:10.1103/PhysRevB.67.104508.

Dvorkin, J., J. Walls, T. Taner, N. Derzhi, and G. Mavko (2003), Attenuation at patchy saturation—A model, paper presented at EAGE 65th Conference and Exibition, Eur. Assoc. of Geosci. and Eng., Stavanger, Norway, 2–5 June.

Faul, U. H., J. D. Fitz Gerald, and I. Jackson (2004), Shear wave attenuation and dispersion in melt-bearing olivine polycrystals: 2. Microstructural interpretation and seismological implications, *J. Geophys. Res.*, *109*, B06202, doi:10.1029/2003JB002407.

Gusev, V. E., W. Lauriks, and J. Thoen (1998), Dispersion of nonlineaeity, nonlinear dispersion, and absorption of sound in micro-inhomogeneous materials, *J. Acoust. Soc. Am.*, *103*(6), 3216–3226, doi:10.1121/1.423037.

Guyer, R. A., and P. A. Johnson (1999), Nonlinear mesoscopic elasticity: Evidence for a new class of materials, *Phys. Today*, *52*(4), 30–36, doi:10.1063/1.882648.

Guyer, R. A., K. R. McCall, and G. N. Boitnott (1995), Hysteresis, discrete memory and nonlinear wave propagation in rock: A new paradigm, *Phys. Rev. Lett.*, *74*(17), 3491–3494, doi:10.1103/PhysRevLett.74.3491.

Jackson, I., J. D. Fitz Gerald, U. H. Faul, and B. H. Tan (2002), Grain-size sensitive seismic wave attenuation in polycrystalline olivine, *J. Geophys. Res.*, *107*(B12), 2360, doi:10.1029/2001JB001225.

Johnson, P. A., B. Zinszner, and P. N. J. Rasolofosoan (1996), Resonance and elastic nonlinear phenomena in rock, *J. Geophys. Res.*, *101*, 11,553–11,564, doi:10.1029/96JB00647.

Johnston, D. H., and M. N. Toksoz (1980a), Thermal cracking and amplitude dependent attenuation, *J. Geophys. Res.*, *85*, 937–942, doi:10.1029/JB085iB02p00937.

Johnston, D. H., and M. N. Toksoz (1980b), Ultrasonic P and S wave attenuation in dry and saturated rocks under pressure, *J. Geophys. Res.*, *85*, 925–936, doi:10.1029/JB085iB02p00925.

Jones, S. M. (1995), Velocity and quality factors of sedimentary rocks at low and high effective pressures, *Geophys. J. Int.*, *123*, 774–780, doi:10.1111/j.1365-246X.1995.tb06889.x.

Mashinskii, E. I. (2001), Nonlinearity of a quasi-static stress-strain relation: The dependence on the level of mechanical energy, *Geofizika*, *2*, 37–41.

Mashinskii, E. I. (2004), The variants of the strain-amplitude dependence of elastic wave velocities in the rocks under pressure, *J. Geophys. Eng.*, *1*, 295–306, doi:10.1088/1742-2132/1/4/008.

Mashinskii, E. I. (2005a), Experimental study of the amplitude effect on wave velocity and attenuation in consolidated rocks under confining pressure, *J. Geophys. Eng.*, *2*, 199–212, doi:10.1088/1742-2132/2/3/004.

Mashinskii, E. I. (2005b), Non-linear stress-strain relation in sedimentary rocks and its effect on seismic wave velocity, *Geophysica*, *41*(1), 3–17.

Mashinskii, E. I. (2006), Nonlinear amplitude-frequency characteristics of attenuation in rock under pressure, *J. Geophys. Eng.*, *3*, 291–306, doi:10.1088/1742-2132/3/4/001.

Mashinskii, E. I. (2007), Effect of strain amplitude on the relaxation spectra of attenuation in the dry and saturated sandstone under pressure, *J. Geophys. Eng.*, *4*, 194–203, doi:10.1088/1742-2132/4/2/008.

Mashinskii, E. I., and G. N. D'yakov (1999), Amplitude-dependent attenuation of pulse signals in rocks, *Izv. Phys. Solid Earth*, *35*, 937–940.

Mashinskii, E. I., V. Z. Koksharov, and Y. A. Nefedkin (1999), Amplitude-dependent effects in the range of small seismic strains, *Geol. Geofiz.*, *40*, 611–618.

Mashinsky, E. I. (1994), Quasi-micro-plasticity processes and nonlinear seismicity, *Phys. Solid Earth*, *30*, 97–102.

Mavko, G. M. (1979), Friction attenuation: An inherent amplitude dependence, *J. Geophys. Res.*, *84*, 4769–4775, doi:10.1029/JB084iB09p04769.

Mavko, G., and J. Dvorkin (2005), P-wave Attenuation in reservoir and non-reservoir rock, paper presented at EAGE 67th Conference and Exhibition, Eur. Assoc. of Geosci. and Eng., Madrid, Spain, 13–16 June.

Murphy, F. M., K. W. Winkler, and R. L. Kleinberg (1986), Acoustic relaxation in sedimentary rocks: Dependence on grain contacts and fluid saturation, *Geophysics*, *51*(3), 757–766, doi:10.1190/1.1442128.

Ostrovsky, L. A., and P. A. Johnson (2001), Dynamic nonlinear elasticity in geomaterials, *Riv. Nuovo Cimento*, *24*(4), 7.

Prasad, M., and M. H. Manghnani (1997), Effect of pore and differential pressure on compressional wave velocity and quality factor in Berea and Michigan sandstones, *Geophysics*, *62*(4), 1163–1176, doi:10.1190/1.1444217.

Spencer, J. W. (1981), Stress relaxation at low frequencies in fluid-saturated rocks: Attenuation and modulus dispersion, *J. Geophys. Res.*, *86*, 1803–1812, doi:10.1029/JB086iB03p01803.

Stewart, R. R., M. N. Toksoz, and A. Timur (1983), Strain dependent attenuation: Observations and a proposed mechanism, *J. Geophys. Res.*, *88*, 546–554, doi:10.1029/JB088iB01p00546.

Taylor, S. R., and R. J. Knight (2003), Incorporating mechanisms of fluid pressure relaxation into inclusion-based models of elastic wave velocities, *Geophysics*, *68*(4), 1173–1181, doi:10.1190/1.1598110.

Tutuncu, A. N., A. L. Podio, and M. M. Sharma (1994a), An experimental investigation of factors influencing compressional- and shear-wave velocities and attenuations in tight gas sandstones, *Geophysics*, *59*(1), 77–86, doi:10.1190/1.1443536.

Tutuncu, A. N., A. L. Podio, and M. M. Sharma (1994b), Strain amplitude and stress dependence of static moduli in sandstones and limestones, in *Rock Mechanics: Models and Measurements: Challenges From Industry*, edited by P. Nelson and S. Laubach, pp. 489–496, A. A. Balkema, Rotterdam.

Tutuncu, A. N., A. L. Podio, A. R. Gregory, and M. M. Sharma (1998), Nonlinear viscoelastic behavior of sedimentary rocks. Part I: Effect of frequency and strain amplitude, *Geophysics*, *63*(1), 184–194.

Winkler, K. W. (1983), Frequency dependent ultrasonic properties of high-porosity sandstones, *J. Geophys. Res.*, *88*, 9493–9499, doi:10.1029/JB088iB11p09493.

Winkler, K. W. (1985), Dispersion analysis of velocity and attenuation in Berea sandstone, *J. Geophys. Res.*, *90*, 6793–6800, doi:10.1029/JB090iB08p06793.

Winkler, K. W., and T. J. Plona (1982), Technique for measuring ultrasonic velocity and attenuation spectra in rocks under pressure, *J. Geophys. Res.*, *87*, 10,776–10,780, doi:10.1029/JB087iB13p10776.

Winkler, K. W., A. Nur, and M. Gladwin (1979), Friction and seismic attenuation in rock, *Nature*, *277*, 528–531, doi:10.1038/277528a0.

Zaitsev, V. Y., and L. A. Matveev (2006), Strain-amplitude dependent dissipation in linearly dissipative and nonlinear elastic microghomogeneous media, *Russ. Geol. Geophys.*, *47*(5), 695–710.

Zaitsev, V. Y., and P. Sas (2000), Dissipation in microinhomogeneous solids: Inherent amplitude-dependent losses of a non-hysteretical and non-frictional type, *Acta Acustica*, *86*, 429–445.

Zaitsev, V. Y., V. E. Nazarov, and V. I. Talanov (1999), Experimental study of the self-action of seismoacoustic waves, *Acoust. Phys.*, *45*(6), 720–726.

E. I. Mashinskii, Institute of Petroleum Geology and Geophysics, Siberian Branch of the RAS, prospect Akademika Koptyuga 3, Novosibirsk, 630090, Russia. (MashinskiiEI@ipgg.nsc.ru)